Progress in Physics (70)

Chiral twist in the story of mesoscopic magnetic systems

Aleš Hrabec [1,2,3], Zhaochu Luo [1,2], T. Phuong Dao [1,2,3], Pietro Gambardella [3], Laura J. Heyderman [1,2]
*[1] Laboratory for Mesoscopic Systems, Department of Materials, ETH Zürich, 8093 Zürich*
[2] Paul Scherrer Institut, 5232 Villigen PSI
[3] Laboratory for Magnetism and Interface Physics, Department of Materials, ETH Zürich, 8093 Zürich

Chiral coupling on the atomic scale

The Heisenberg exchange interaction lies at the heart of magnetism since it is responsible for the collinear alignment of the magnetic moments of neighbouring atoms. It is usually represented by the Hamiltonian $J\,\boldsymbol{m}_i \cdot \boldsymbol{m}_j$, where the sign of the exchange constant J dictates whether the magnetic order is ferromagnetic or antiferromagnetic in nature. In the 1950s, based on symmetry arguments, Igor Dzyaloshinskii and Toru Moriya deduced a new type of interaction between two neighbouring spins leading to their non-collinear alignment. The key ingredients are a strong spin–orbit coupling,

which links the electron spin to the atomic lattice, and a broken structure-inversion symmetry that naturally occurs at surfaces and interfaces. This interaction is generally expressed as $-\boldsymbol{D}_{ij} \cdot (\boldsymbol{m}_i \times \boldsymbol{m}_j)$ where D is the Dzyaloshinskii-Moriya interaction (DMI) constant and its vector orientation reflects the symmetry of the system [1]. Experimental signatures of this interaction were first revealed in weak ferromagnets and antiferromagnets, and seemed to be only relevant for a restricted class of materials [2,3]. However, with the advent of ultrathin magnetic films and their implementation in spintronics, it was realised that this interaction can play a key role in technologically relevant systems [4,5].
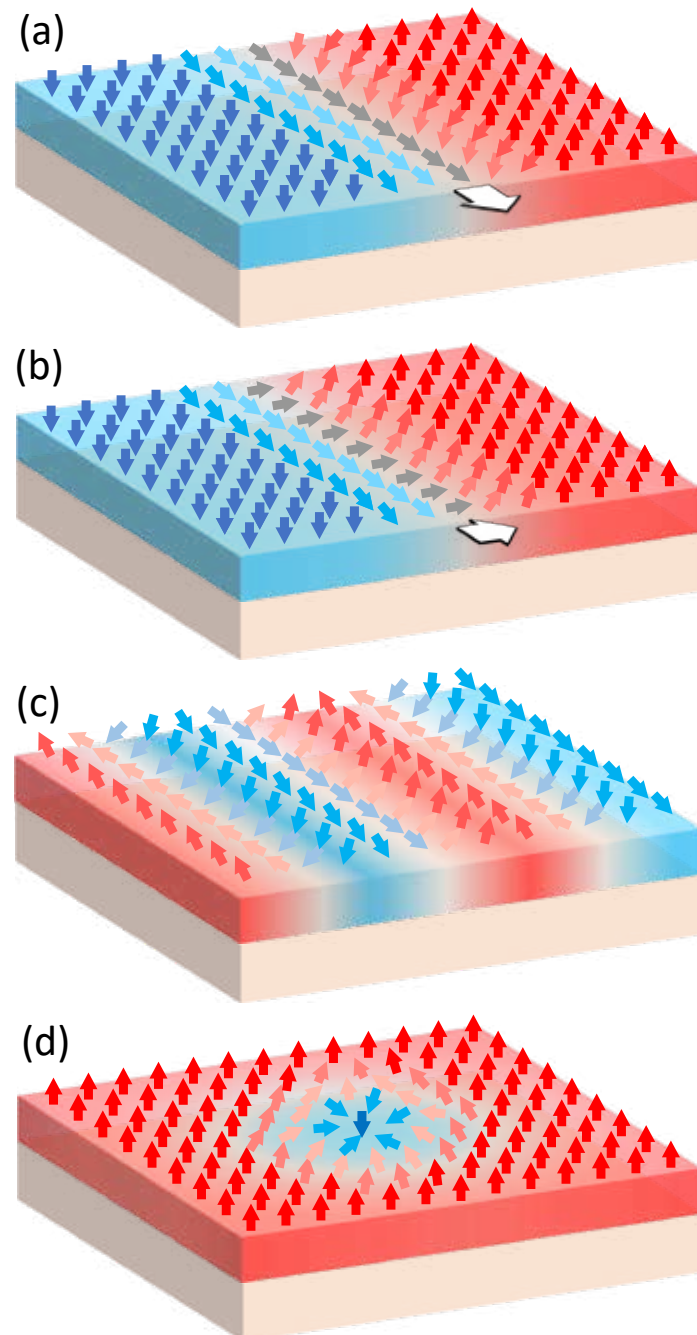
In thin films, the interfacial DMI can cause a twist of magnetic domain walls from a magnetostatically stable Bloch configuration (Fig.1a) into a Néel configuration of a fixed chirality (Fig. 1b), and ultimately stabilize non-collinear magnetic order such as spin spirals or skyrmions [8] (Fig. 1c and d). This seemingly unimportant twist has profound consequences on the domain wall dynamics [9]. Their miniscule size and sensitivity to the electric currents, make domain walls attractive as nanoscopic information carriers in data storage devices [7]. We show here how the DMI can be tuned and exploited to create artificial magnetic systems on different length scales, opening new opportunities to study topological spin textures and to control the magnetization dynamics of nanoscale magnets.

Chiral coupling on mesoscopic scale

The size of the magnetic textures such as domain walls, skyrmions or cycloids is naturally defined in magnetic materials and thus limited by the interplay between the competing magnetic energies. Here, we exploit these natural length scales in artificial mesoscopic structures, placing the $-\boldsymbol{D}_{ij} \cdot (\boldsymbol{m}_i \times \boldsymbol{m}_j)$ twist in particular locations to give novel magnetic configurations and effects. The artificial structures are composed of regions with out-of-plane and in-plane magnetic anisotropies as illustrated in Fig. 2a, fabricated using advanced lithography techniques. Pt(6 nm)\Co(1.6 nm)\Al films were deposited onto silicon substrates using magnetron sputtering and consequently patterned into nanoscale islands. Due to the shape anisotropy and a low effective in-

(a)

(b)

(c)

(d)

Figure 1: Magnetic domain walls in out-of-plane magnetized films. (a) Films in the absence of DMI contain achiral Bloch walls stabilized by internal domain wall anisotropy. In such a case, the magnetization in the centre of a domain wall lies along the domain wall. (b) If DMI is present and is high enough to overcome the internal domain wall anisotropy, a Néel wall of a fixed chirality (i.e. fixed sense of rotation as one goes across the magnetic texture) becomes stable. Here, the magnetization in the centre of the domain wall is perpendicular to the domain wall. If DMI is strong enough, it can bring the ground state into (c) a spin spiral or (d) a skyrmions state.

terfacial anisotropy arising from the lower Pt\Co interface, the magnetization orientation is confined in the film plane. In order to obtain perpendicular magnetic anisotropy, we add a Co\AlO$_x$ upper interface [10]. This can be achieved by a controlled oxidation of the aluminium top layer. A selective oxidation is realized using a mask during the oxidation process that protects the parts of the structure where the magnetic easy axis remains within the film plane. Crucially, due to the combination of high spin-orbit coupling and broken inversion symmetry, the Pt\Co interface serves as a source of the aforementioned DMI. This interaction provides an essential connection between the in-plane and out-of-plane magnetized parts of the structure, which would otherwise only be coupled via non-chiral exchange and dipolar interactions.
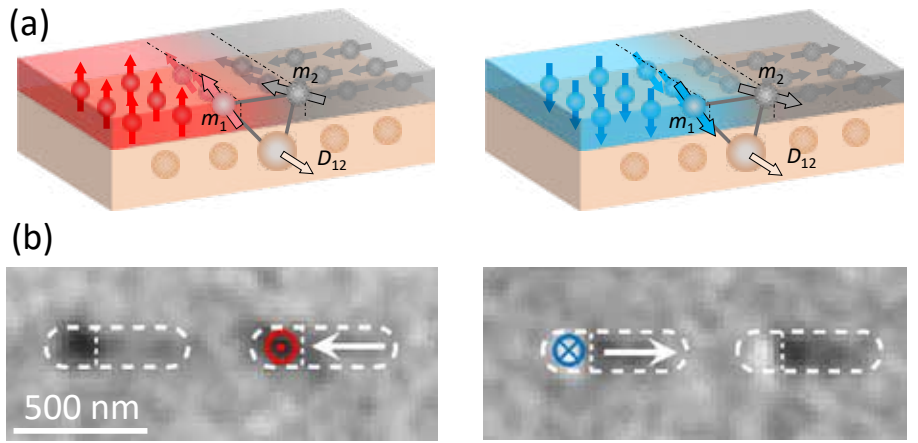

Figure 2: (a) Schematics of the hybrid magnetic systems composed of coupled out-of-plane and in-plane magnetized regions. DMI in Pt\Co layers prefers a left-handed chiral ordering of the magnetization, i.e. up-left (left panel) or down-right (right panel). (b) X-PEEM images corresponding to the magnetization ordering depicted in (a). The dark and bright contrast in the out-of-plane regions corresponds to ↑ and ↓ states, respectively. The dark and light grey contrast in the IP magnetized parts corresponds to → and ← magnetization, respectively.

Due to the size of the fabricated patterns, which are below resolution of conventional microscopy techniques, we investigated the chirally coupled structures with x-ray photoemission electron microscopy (X-PEEM). Since X-PEEM is sensitive to the projection of the magnetization direction along the incident x-ray direction, the contrast in Fig. 2b simultaneously provides information on the orientation of the out-of-plane and in-plane magnetized parts of the structure. Here, the magnetic state has been initialized with an in-plane magnetic field prior to the imaging. As shown in Fig. 2b, when the magnetization of the in-plane element M_{IP} points to the left (right), the adjacent out-of-plane magnetized element M_{OOP} points up (down). This confirms the chiral nature of the DMI, the coupling between the two elements and agrees with the expected left handedness arising at the Pt\Co interface. Therefore, the DMI not only has the power to twist magnetic moments at the atomic length scale as demonstrated previously but can also be effective in larger structures where the in-plane and out-of-plane magnetized regions can be represented by a macroscopic magnetic moment $-\boldsymbol{D} \cdot (\boldsymbol{M}_{IP} \times \boldsymbol{M}_{OOP})$.

All-electric switching and readout

In order to proceed towards technologically relevant devices where full electric magnetization control is essential for next-generation data storage devices, we fabricated hybrid out-of-plane/in-plane magnetized structures on top of Pt cross structures (Fig. 3a), where the state of the out-of-plane magnetized part can be detected electrically. In particular, the anomalous Hall effect is used to detect the z-component (i.e. M_{OOP}) of the magnetization via the Hall resistivity R_{xy}. Prior to the application of the H_z field, the state of M_{IP} is preset with a positive or negative H_y field, respectively. The DMI effective field localized at the interface between the out-of-plane and in-plane magnetized regions contains an out-of-plane component acting here effectively as an exchange bias. Therefore the positive and negative shift of the hysteresis loops seen in Fig. 3b reflects the fact that the sign of the effective field [5,11,12] is re-
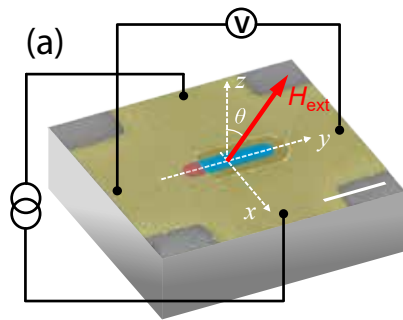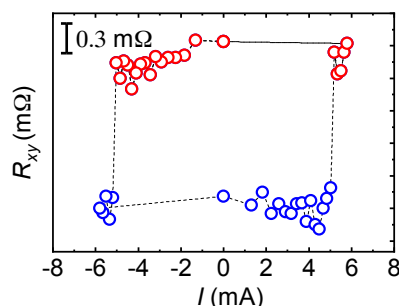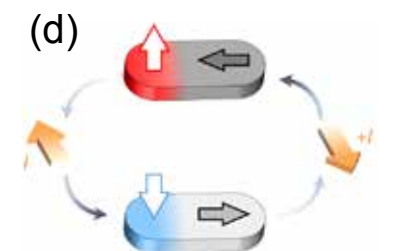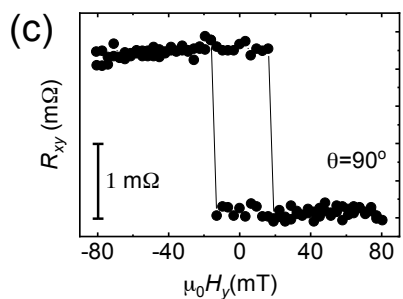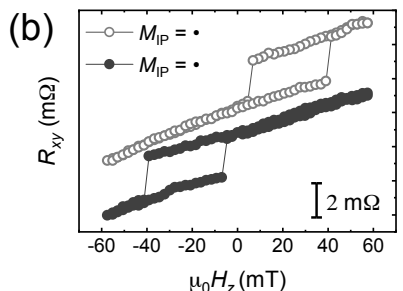

Figure 3: (a) Schematic of a hybrid in-plane/out-of-plane structure fabricated on top of a Pt cross (yellow) designed for anomalous Hall effect measurements. Here the electric current is applied along the short axis of the island and the anomalous Hall effect resistivity R_{xy} is measured transversally. (b) Anomalous Hall effect resistivity as a function of an out-of-plane magnetic field for the case where the magnetic state of the in-plane magnetized part of the island has been preset by a positive (empty circles) or negative (full circles) in-plane magnetic field. The hysteresis loops are biased due to an effective field arising at the boundary between the out-of-plane and in-plane magnetized parts. (c) Anomalous Hall effect resistivity measured as a function of an in-plane magnetic field reveals simultaneous switching of the out-of-plane magnetization. (d) The magnetic state can be controlled by an electric current whose polarity sets the state. The anomalous Hall effect resistivity measurements as a function of electric current pulse amplitude reveal that the magnetic state can be switched with a current of 5.5 mA, which corresponds to a current density of $J \approx 4.7 \times 10^{11}$ A/m^2.
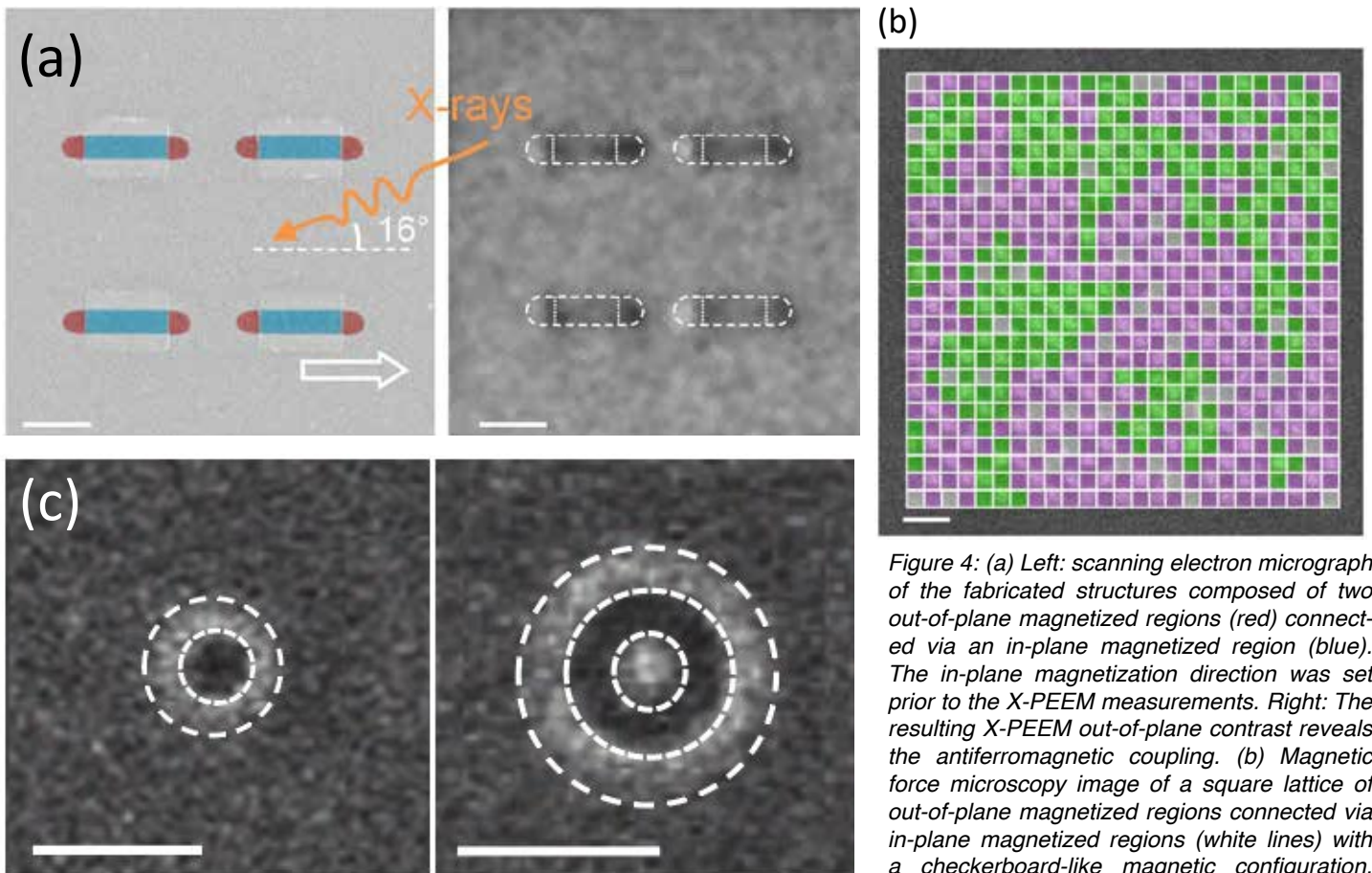
Figure 4: (a) Left: scanning electron micrograph of the fabricated structures composed of two out-of-plane magnetized regions (red) connected via an in-plane magnetized region (blue). The in-plane magnetization direction was set prior to the X-PEEM measurements. Right: The resulting X-PEEM out-of-plane contrast reveals the antiferromagnetic coupling. (b) Magnetic force microscopy image of a square lattice of out-of-plane magnetized regions connected via in-plane magnetized regions (white lines) with a checkerboard-like magnetic configuration. There are two energetically equivalent antiferro-magnetic domains highlighted in green and purple. (c) Magnetic force microscopy image of a skyrmion-like magnetic state, which occurs as a result of chiral coupling mediated by in-plane magnetized rings (dashed circles). The topological charge can be altered from ±1 to 0 by adding another out-of-plane ring. All scale bars correspond to 500 nm.

versed for different initial configurations of the in-plane region. This reveals the power of the chiral coupling: the DMI is strong enough to spontaneously form the chiral states upon releasing the external magnetic fields. Therefore, setting the in-plane magnetization affects the out-of-plane magnetization reversal. In additon, the magnetic state of the out-of-plane magnetized regions can be controlled by the application of the in-plane magnetic field (Fig. 3c).

When an electric current is applied, the Pt underlayer also provides a source of a net spin current generated via the spin Hall effect, which offers a means to manipulate the magnetic state of the structures. It has been previously shown that the magnetic state of in-plane or out-of-plane magnetized magnets can be controlled by spin-orbit torques arising from the interaction between the absorbed spin current and the local current [13,14]. However, to achieve magnetization switching with an electric current, an additional symmetry-breaking is required. This is usually achieved by applying an additional external in-plane magnetic field, which is not desirable for device applications. In our case, the symmetry is intrinsically reduced by the presence of the in-plane magnetized part enabling the deterministic spin-orbit torque-induced switching. The spin-orbit torques thus cause simultaneous switching of the out-of-plane and in-plane regions. These can be switched back and forth by reversing the polarity of the applied electric current. This is demonstrated by the hysteresis loop presented in Fig. 3d and, in order to achieve the field-free current-induced switching, a current density of $J \approx 4.7 \times 10^{11}$ A/m^2 is required. This demonstrated magnetic field-free, all-electrical writing and readout of the magnetic state opens opportunities to design new data storage and memory devices. For example, the lateral chiral coupling can be used to realize magnetic logic devices controlled purely by an electric current [15].

Chiral coupling in complex geometries

The potential of the lateral chiral coupling can also be implemented in more complex two-dimensional systems of various geometries. Structures with two out-of-plane magnetized regions (in red) that coupled antiferromagnetically across an in-plane region (in blue) are shown in Fig. 4a. Once the magnetic state of the in-plane region is set, the two out-of-plane elements order in an antiferromagnetic fashion, mimicking the negative atomistic Heisenberg exchange interaction on a mesoscopic scale. Magnetic couplings in vertically layered structures such as exchange bias or Ruderman-Kittel-Kasuya-Yosida coupling play a key role in magnetic data storage devices. However, the magnetic coupling in laterally defined structures has so far been limited to dipolar interactions, which are very small in ultrathin magnetic films currently used in spintronics. The lateral chiral coupling effect, which is effective also on a mesoscopic scale, provides a robust alternative to the systems coupled via dipolar interaction [16].

The lateral antiferromagnetic coupling demonstrated in simple building blocks shown in Fig. 4a can be extended into two dimensions by ordering these blocks into a square lattice. Such a lattice is composed of out-of-plane magnet-

ized squares connected via narrow in-plane magnetized connectors mediating the chiral coupling and provides a mesoscopic analogue to a correlated Ising-like spin system. The resulting checkerboard-like magnetic state, captured by magnetic force microscopy, is shown in Fig. 4b. The alternating black and white contrast reflects the fact that the out-of-plane elements are ordered in an antiferromagnetic fashion. Nevertheless, there are two energetically equivalent magnetic configurations (up-down-up-down or down-up-down-up), which results in the formation of two different antiferromagnetic domains highlighted in green and purple. This provides an interesting development in the field of artificial spin systems [17,18].

The concept of chiral coupling can be further implemented in curved geometries as demonstrated by the skyrmion-like structures shown in Fig. 4c, which are composed of different numbers of in-plane magnetized rings (dashed lines). The alternating even and odd number of in-plane rings changes the topological charge of the resulting magnetic texture. For an odd number of in-plane rings, the topological charge is +1 or -1, depending on the orientation of the magnetization of the central region. For an even number of in-plane rings, the topological charge is 0, and the so-called 2π skyrmions are topologically equivalent to a ferromagnetic state, i.e. it can be simply unrolled to a simple ferromagnetic state.

Although here the lateral coupling has been produced in a controllable way by spatially tailoring the local anisotropies, it may be possible to find similar effects in inhomogeneous magnetic systems with broken inversion symmetry, for example, in magnetic systems near the spin reorientation transition [19] or in multilayer magnetic films [20,21].

[1] Moriya, T. Anisotropic Superexchange Interaction and Weak Ferromagnetism. *Phys. Rev.* **120,** 91–98 (1960).
[2] Moriya, T. New Mechanism of Anisotropic Superexchange Interaction. *Phys. Rev. Lett.* **4**, 228–230 (1960).
[3] Dzyaloshinsky, I. A thermodynamic theory of "weak" ferromagnetism of antiferromagnetics. *J. Phys. Chem. Solids* **4**, 241–255 (1958).
[4] Crépieux, A. & Lacroix, C. Dzyaloshinsky–Moriya interactions induced by symmetry breaking at a surface. *J. Magn. Magn. Mater.* **182**, 341–349 (1998).
[5] Thiaville, A., Rohart, S., Jué, É., Cros, V. & Fert, A. Dynamics of Dzyaloshinskii domain walls in ultrathin magnetic films. *Europhys. Lett.* **100**, 57002 (2012).
[6] Parkin, S. S. P., Hayashi, M. & Thomas, L. Magnetic domain-wall racetrack memory. *Science* **320**, 190–194 (2008).
[7] P. del Real, R., Raposo, V., Martinez, E. & Hayashi, M. Current-Induced Generation and Synchronous Motion of Highly Packed Coupled Chiral Domain Walls. *Nano Lett.* **17**, 1814–1818 (2017).
[8] Bode, M. *et al.* Chiral magnetic order at surfaces driven by inversion asymmetry. *Nature* **447**, 190–193 (2007).
[9] Emori, S., Bauer, U., Ahn, S.-M., Martinez, E. & Beach, G. S. D. Current-driven dynamics of chiral ferromagnetic domain walls. *Nat. Mater.* **12**, 611–616 (2013).
[10] Manchon, A. *et al.* Analysis of oxygen induced anisotropy crossover in Pt/Co/MO$_x$ trilayers. *J. Appl. Phys.* **104**, 043914 (2008).
[11] Rohart, S. & Thiaville, A. Skyrmion confinement in ultrathin film nanostructures in the presence of Dzyaloshinskii-Moriya interaction. *Phys. Rev. B* **88**, 184422 (2013).
[12] Hrabec, A. *et al.* Measuring and tailoring the Dzyaloshinskii-Moriya interaction in perpendicularly magnetized thin films. *Phys. Rev. B* **90**, 1–5 (2014).
[13] Miron, I. M. *et al.* Perpendicular switching of a single ferromagnetic layer induced by in-plane current injection. *Nature* **476**, 189–193 (2011).
[14] Fukami, S., Anekawa, T., Zhang, C. & Ohno, H. A spin–orbit torque switching scheme with collinear magnetic easy axis and current configuration. *Nat. Nanotechnol.* **11**, 621–625 (2016).
[15] Dao, T. P. *et al.* Chiral Domain Wall Injector Driven by Spin–Orbit Torques. *Nano Lett.* **19**, 5930–5937 (2019).
[16] Luo, Z. *et al.* Chirally coupled nanomagnets. *Science* **363**, 1435–1439 (2019).
[17] Heyderman, L. J. & Stamps, R. L. Artificial ferroic systems: novel functionality from structure, interactions and dynamics. *J. Phys. Condens. Matter* **25**, 363201 (2013).
[18] Nisoli, C., Moessner, R. & Schiffer, P. Colloquium: Artificial spin ice: Designing and imaging magnetic frustration. *Rev. Mod. Phys.* **85**, 1473–1490 (2013).
[19] Vijayakumar, J. *et al.* Electric field control of magnetism in Si$_3$N$_4$ gated Pt/Co/Pt heterostructures. *J. Appl. Phys.* **125**, 114101 (2019).
[20] Hauschild, J., Gradmann, U. & Elmers, H. J. Perpendicular magnetization and dipolar antiferromagnetism in double layer nanostripe arrays of Fe(110) on W(110). *Appl. Phys. Lett.* **72**, 3211–3213 (1998).
[21] Friesen, C. *et al.* Magneto-Seebeck tunneling on the atomic scale. *Science* **363**, 1065–1067 (2019).